



Cite this: *Soft Matter*, 2017, 13, 608

# Interfacial properties and emulsification performance of thylakoid membrane fragments

A. Tamayo Tenorio,<sup>a</sup> E. W. M. de Jong,<sup>a</sup> C. V. Nikiforidis,<sup>ab</sup> R. M. Boom<sup>a</sup> and A. J. van der Goot<sup>\*a</sup>

Thylakoids membranes are sophisticated, dynamic structures found in plant leaves, composed of protein complexes in a dynamic lipid matrix. The interfacial absorption dynamics and viscoelasticity of thylakoid membranes fragments were measured to assess the properties of the interfacial layer and to elucidate an emulsifying mechanism that includes the role of thylakoid's composition and 3D structure. Thylakoid membranes were extracted from sugar beet leaves by a series of buffer washing, filtration and centrifugation. The extract containing the intact thylakoid membranes was suspended in water through high-pressure homogenisation, which disrupted the structure into membrane fragments. Thylakoid fragments showed surface and interfacial behaviour similar to soft particles or Pickering stabilizers with slow adsorption kinetics. After adsorption, an elastic and stable thin film was formed, indicating formation of new interactions between adjacent thylakoid fragments. In an emulsion, thylakoid fragments stabilised oil droplets against coalescence, despite droplet aggregation occurring already during emulsification. Droplet aggregation occurred by steric and electrostatic bridging, which in turn forms a 3D network where the oil droplets are immobilised, preventing further droplet coalescence or aggregation. It was concluded that both composition and structure of thylakoid fragments determine their emulsifying properties, conferring potential for encapsulation systems, where the search for natural materials is gaining more attention.

Received 27th September 2016,  
Accepted 5th December 2016

DOI: 10.1039/c6sm02195f

[www.rsc.org/softmatter](http://www.rsc.org/softmatter)

## Introduction

Plant leaves are rich in thylakoids; membrane structures that are responsible for the photosynthetic reactions. These membranes structures are one of the most abundant biological membranes in nature and are the most complex regarding composition, structure and function.<sup>1</sup> Thylakoid membranes structures comprise protein complexes in a dynamic lipid matrix, which enable the efficient conversion of light energy into chemical energy.

Thylakoids are located in the chloroplasts of green leaves in the form of stacks (granal thylakoids) that are interconnected by non-stacked lamellae (stromal thylakoids).<sup>2</sup> These two domains are organized in a complex 3D network that is facilitated by the special composition of thylakoid membranes.<sup>3</sup> Thylakoids consist of 60–65 wt% proteins and 35–40 wt% lipids.<sup>4–6</sup> The thylakoid proteins are protein complexes that are unevenly distributed within the membrane; their highly specialised functions explain their complex composition and 3D arrangement.

Unlike most eukaryotic membranes, thylakoid lipids are poor in phospholipids (~5–12 wt%), but composed of galactolipids like monogalactosyldiacylglycerol (MGDG; ~50%), digalactosyldiacylglycerol (DGDG; ~30%), and sulfoquinovosyldiacylglycerol (SQDG; ~5–12%).<sup>7</sup> Both proteins and lipids in the thylakoid membranes adopt an intricate but dynamic structure,<sup>1</sup> showing transitions between conformations (*e.g.* bilayer to hexagonal phases) to enable enzyme activity<sup>7</sup> or to respond to stress conditions.<sup>4</sup>

Their sophisticated and dynamic structure motivates the study of thylakoids as a biobased material for valuable applications, as a response to the current need for resource optimisation and demand for natural ingredients. The use of more intact parts present in biomass is a promising route to reach those goals. Thylakoids are known to stabilize oil droplets (emulsifiers) and exhibit satiation effect upon consumption,<sup>8,9</sup> which has been attributed to slow digestion rate of the thylakoids and the subsequent release of satiety hormones, together with lipolysis inhibition.<sup>9</sup> Both the emulsifying ability and slow digestibility make thylakoids an excellent candidate as stabilizers of oil capsules for targeted release of healthy compounds. A further understanding of their functional properties may lead to advanced applications in foods, cosmetics and pharmaceuticals.

<sup>a</sup> Food Process Engineering Group, Wageningen University, P.O. Box 17, 6700 AA Wageningen, The Netherlands. E-mail: [Atzejan.vandergoot@wur.nl](mailto:Atzejan.vandergoot@wur.nl)

<sup>b</sup> Biobased Chemistry and Technology Group, Wageningen University, P.O. Box 17, 6700 AA Wageningen, The Netherlands



Little is known about the emulsifying mechanism and interfacial properties of thylakoid membranes<sup>8,10</sup> and no literature reports on how these aspects are linked to their composition and 3D structure. It can be easily hypothesized that both proteins and lipids play an important role in droplet stabilisation. The interfacial properties of the protein/lipid complexes can be analysed based on adsorption dynamics and dilatational rheology analysis. The adsorption dynamics provide a deeper understanding of the kinetics of molecules towards an interface, while compression/expansion measurements define the interfacial viscoelasticity of the adsorbed layer through the dilatational modulus.

In this study, we extracted thylakoid membranes from sugar beet leaves based on protocols developed for photosynthesis analysis, rendering a rather pure thylakoid isolate. The characterisation of the isolated thylakoids focused on their technological functionality as emulsifiers. Their interfacial absorption and viscoelasticity were measured to assess the properties of the interfacial film. These fundamental measurements were further used to build a hypothesis on the emulsification mechanism with thylakoids as emulsifying structures. The discussion describes the possible relations of the interfacial behaviour with the thylakoid's composition and native 3D arrangements. Moreover, extraction of thylakoids from side streams like sugar beet leaves, constitutes a high value application for leafy biomass that takes advantage of functional structures present in nature.<sup>11</sup>

## Experimental section

### Materials

Agarose, EDTA (Ethylenediaminetetraacetic acid), glutaraldehyde, hydrochloric acid, Hepes (4-(2-hydroxyethyl)-1-piperazineethanesulfonic acid), osmium oxide (OsO<sub>4</sub>), potassium ferricyanide, sodium cacodylate, sodium chloride (NaCl), sodium hydroxide (NaOH), Spurr resin and tricine were obtained from Sigma Aldrich (St. Louis, MO, USA). Magnesium chloride (MgCl<sub>2</sub>), potassium hydroxide (KOH) and D-sorbitol were obtained from Merck (Darmstadt, Germany). Sunflower oil was obtained from a local supermarket and used without further purification, except for interfacial tension measurements where the oil was stripped by means of alumina (MP Alumina N-Super I, MP Biomedicals, Germany) as described by Berton *et al.*<sup>12</sup> Milli-Q water was used in all the experiments.

### Thylakoids extraction

Sugar beet leaves from mature plants were harvested prior to thylakoid extraction from a sugar beet production field in Wageningen, The Netherlands. Only leaf blades were used for extraction. The thylakoid extraction protocol was based on that of Casazza *et al.*<sup>13</sup> and Joly & Carpentier<sup>14</sup> and is depicted in Fig. 1. The fresh leaves were blended in a kitchen blender Waring 8011EG (Waring, Torrington, USA), three times for 6 s with buffer 1 (0.4 M sorbitol, 5 mM MgCl<sub>2</sub>, 20 mM tricine/KOH at pH 7.8, 5 mM EDTA), in a leaf-to-buffer weight ratio of 1:5. The homogenate was passed through four layers of cheese cloth and the retentate was discarded. After centrifugation (10 000g,

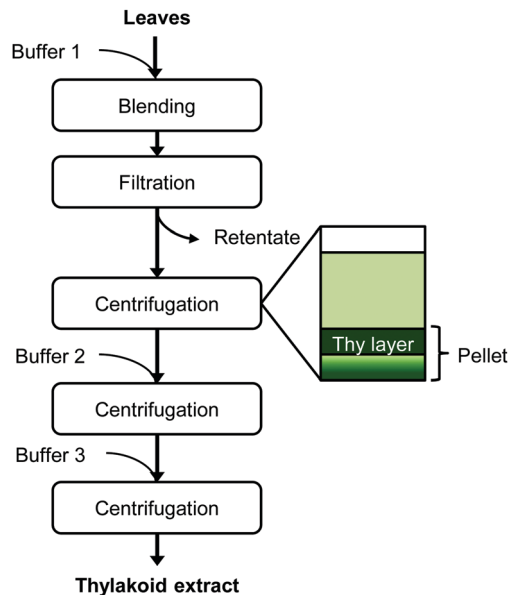


Fig. 1 Extraction protocol of thylakoid membranes from leaves. At each centrifugation step, only the thylakoid-containing layer was recovered to continue the protocol. Thy = thylakoids.

30 min, 4 °C), the top layer of the pellet was recovered and re-suspended in buffer 2 (0.3 M sorbitol, 5 mM MgCl<sub>2</sub>, 20 mM tricine/KOH at pH 7.8, 2.5 mM EDTA). After a second centrifugation (10 000g, 30 min, 4 °C), the top part of the pellet was recovered and re-suspended in buffer 3 (3.5 mM EDTA, 20 mM Hepes/KOH pH 7.5). After a final centrifugation at the same conditions, the top part of the pellet was collected and stored at −18 °C. This pellet fraction is referred to as “thylakoid extract”.

### Extract composition

The moisture content was determined gravimetrically with samples that were dried in an oven at 50 °C for 48 h. The nitrogen content of dry samples was measured in duplicate by Dumas analysis (NA 2100 Nitrogen and Protein Analyser, ThermoQuest-CE Instruments, Rodeno, Italy). Nitrogen values were converted to protein values using a conversion factor of 6.25 with methionine as standard. Total dietary fibre was determined with a Megazyme assay kit (Megazyme International, Bray, Ireland) according to AACC method 32-05.01.<sup>15</sup> Ash and fat content were determined with AACC method 08-01 and method 30-25, respectively.<sup>16,17</sup>

### Zeta potential measurements

The ζ-potential was measured in triplicate as a function of pH by a Zetasizer (Malvern Instruments, Worcestershire, UK) with an autotitrator (Malvern Instruments, Worcestershire, UK) at pH between 2.0–10.0. A thylakoid dispersion (0.013 w/v%) was prepared by homogenisation. The samples were diluted ~1000 times in Milli-Q water before analysis.

### Surface tension

Homogenised thylakoid dispersions (0.01, 0.06, 0.13 and 0.25 w/v%) were analysed in triplicate with a Wilhelmy plate (Wägezelle Kraftaufnehmer Q11, HBM, Darmstadt, Germany).



The concentrations refer to the amount of solids. The surface tension measurements were done over 4 h of immersing the plate in the solution; this time interval was appropriate to reach a final steady value ( $\pm 0.5 \text{ mN m}^{-1}$ ) at  $25^\circ\text{C}$ .

### Interfacial tension

The interfacial tension of a thylakoid dispersion (0.001 w/v%) was measured for 24 h in an automated drop tensiometer (Tracker, Teclis-instruments, Tassin, France). A pendant oil drop was formed at the tip of a stainless steel capillary (3 mm diameter), immersed in the thylakoid dispersion. Measurements were made at room temperature and stripped sunflower oil was used. The interfacial tension data measured over time were analysed by fitting to the following equation:

$$\gamma(t) = \gamma_\infty + \gamma_1 e^{-\frac{t}{\tau_1}} + \gamma_2 e^{-\frac{t}{\tau_2}} \quad (1)$$

where  $\gamma_\infty$  represents the surface tension at equilibrium and the exponential terms correspond to the two relaxation modes known for proteins and other macromolecules. The first exponential decay describes the adsorption stage, while the second exponential decay describes the rearrangements of molecules at the interface. Non-linear numerical fitting of (1) to the experimental data was done with the curve fitting tool box of MATLAB software (MathWorks, USA).

### Dilatational viscoelasticity

After reaching the interfacial tension equilibrium, dilatational viscoelasticity measurements were done by interfacial compression and expansion using an amplitude of 5% (v/v) of the initial drop volume and oscillation frequencies of 0.001, 0.005, 0.01, 0.02, 0.05, 0.1 and 0.2 Hz. These measurements provide information on the dynamic properties of the adsorbed surface layer. Once the interface is disturbed, the adsorbed molecules can relieve stress depending on the adsorption or desorption from the bulk solution, resulting in relaxation processes and gradual re-equilibration of the system. The interfacial dilatational modulus ( $E_d$ ) gives a measure of the resistance to surface disturbances and is defined as:

$$E_d = E_d' + E_d'' \quad (2)$$

The real part ( $E_d'$ ) is called the storage modulus and represents the elastic energy stored in the interface (*i.e.* dilatational elasticity). The imaginary part ( $E_d''$ ) is called the loss modulus and accounts for the energy dissipation in the relaxation process (*i.e.* dilatational viscosity).

### Emulsion preparation

Oil-in-water emulsions were prepared by mixing aqueous thylakoid solutions at appropriate concentrations with sunflower oil, using a rotor stator (IKA-Werke GmbH & Co. KG, Staufen, Germany) at 13 500 rpm for 2 min, and subsequently homogenised (Delta Instruments, Drachten, The Netherlands) at 150 bar for 4 min. The sunflower oil concentration was always adjusted to 10% w/w, while the thylakoid concentration was varied (0.03, 0.05, 0.08, 0.10 w/v%). All concentrations refer to

the whole emulsion and not just to the aqueous phase. Emulsions were prepared and analysed in triplicate. The emulsions were stored at  $4^\circ\text{C}$  for stability analyses.

### Emulsion droplet size analysis

The droplet size distributions of thylakoid emulsions was analysed by laser light diffraction with a Mastersizer 2000 (Malvern Instruments, Malvern, UK). High dilution conditions were used to characterize emulsion by dispersing the samples in distilled water. The refractive index ratio used to calculate the oil droplet size distribution was 1.4. Average droplet sizes were characterized in terms of the volume mean diameter:

$$d_{43} = \frac{\sum_i n_i d_i^4}{\sum_i n_i d_i^3} \quad (3)$$

where  $n_i$  is the number of droplets of diameter  $d_i$ . All measurements were made at ambient temperature on three separately prepared samples.

### Microscopy

A leaf cross section, thylakoid extract and thylakoid emulsions were analysed with transmission electron microscopy (TEM). Small leaf pieces ( $1.0 \times 1.5 \text{ mm}$ ) were cut from the mid part of the leaf and fixed for 3 h at room temperature in 3% (v/v) glutaraldehyde in 0.1 M sodium cacodylate buffer (pH 7.2). Thylakoid extract and emulsion were mixed with 3% liquid low melting point agarose in a 1 : 1 ratio. The mix was immediately centrifuged at 5220g, 3 min. The mixture was allowed to solidify at  $0^\circ\text{C}$  and small pieces were cut and fixed for 1.5 h in the same fixative as the leaf pieces. After primary fixation, all samples were washed three times with buffer, successively treated with 1 w/v%  $\text{OsO}_4$  and 1 w/v% potassium ferricyanide in the same buffer for 2 h at room temperature, rinsed in water and dehydrated in a graded ethanol series. The samples were infiltrated with modified Spurr resin mixture (Serva) and cut in ultra-thin (70 nm) sections with an ultra-microtome (Leica Microsystems, Vienna, Austria). The thin sections were analysed with a transmission electron microscope (JEOL, MA, USA). Micrographs were made with a digital camera (Olympus, Veleta).

Thylakoid emulsions were also observed with a light microscope (Axiovert-Zeiss, Gottingen, Germany) fitted with a digital camera (Axio Cam MRc 5, Gottingen, Germany). The samples were observed with and without polarised light.

## Results and discussion

### Characterisation of the thylakoid extract

The thylakoid membrane extraction involved a series of washing and filtration steps. The used buffers and centrifugation steps enabled the separation of intact chloroplasts from the rest of cell components and subsequently, allowed the recovery of thylakoid membranes from the obtained chloroplasts.

### Composition and appearance

The thylakoid extract had an average dry matter content (DM) of 12.6 wt%. The composition of this DM is given in Table 1.



**Table 1** Composition of thylakoid extract on dry basis. The dry matter content was 12.6 wt%. Values are expressed in dry basis.  $n = 3$

Composition	wt% $\pm$ sd
Protein	50.5 $\pm$ 6.5
Dietary fibre	14.2 $\pm$ 3.2
Lipids	17.1 $\pm$ 2.3
Ash	4.6 $\pm$ 1.9

The protein-to-lipid ratio was 75:25, being in line with the thylakoid composition found in literature for other crops.<sup>5,6</sup> This protein-to-lipid ratio is common in energy converting membranes.<sup>7</sup>

To visualise the thylakoids in their native form and after extraction, a leaf cross section and the thylakoid extract were analysed with the aid of TEM. Thylakoid structures were identified inside the chloroplast of the fresh leaf (Fig. 2a, arrows) as well as in the thylakoid extract (Fig. 2b). The thylakoid extract and the fresh leaf contained additional cell structures such as plastoglobules. The latter are thylakoid microdomains responsible for storage and synthesis of lipids<sup>2</sup> and they are identified as dark spherical structures next to the membrane structures.

The extract was a very dense material (semisolid) rich in stacked thylakoid membranes (grana). The stacked thylakoids are 3D structures as depicted in Fig. 2c, and the interconnected supramolecular structures observed with TEM are actually a transversal view of the cylindrical structure. The cylindrical grana stacks are made of membranous discs piled one on top of the other, surrounded by unstacked membranes that are helically bound around the grana.<sup>18</sup> A cartoon of the transversal view of the grana is shown in Fig. 2d, showing the crowded distribution of protein complexes throughout the lipid bilayer. The protein complexes in adjacent membranes are bridged through electrostatic interactions mediated by  $Mg^{2+}$  ions. Thylakoids are negatively charged due to protein phosphorylation and  $Mg^{2+}$  ions can balance the electrostatic repulsion by forming bridges between membranes, leading to membrane stacking.<sup>19,20</sup> The membrane lipids (*i.e.* DGDG) also play a role in stacking by screening the negative charges and through hydrogen bonding between polar

heads of adjacent membranes.<sup>21</sup> Thus thylakoid membranes have the capacity to stack (or aggregate).

### $\zeta$ -Potential measurements

The negative charge of the thylakoid membranes was observed with the  $\zeta$ -potential measurements. A suspension of thylakoids was measured as a function of pH to observe the effect of the environmental pH on the charge of this complex structure. The measurements showed an isoelectric point (IEP) at pH  $4.7 \pm 0.2$  (Fig. 3), which is the same value reported in previous studies for thylakoids from spinach leaves.<sup>22</sup> The charge is mainly a contribution of the protein moieties rather than the lipid moieties for three main reasons: (i) the abundance of proteins compared to lipids; (ii) the lack of charge of the majority of lipids (*i.e.* MGDG, DGDG); and (iii) the constant negative charge of the few polar lipids (*i.e.* PG, SQDG) at all pH ranges. Other charged molecules present in the thylakoids include pigments and minerals that have less pronounced effect on the  $\zeta$ -potential probably due to their even distribution on the thylakoids surface or to their location inside the core of the protein complexes.

In this study, the thylakoid extract was suspended in water by high-pressure homogenisation before any analysis. The thylakoid extract, rich in intact membrane structures (Fig. 2b), was initially not soluble in water and appeared as large clusters ( $\sim 100 \mu\text{m}$ ) under the optical microscope (Fig. 4a). After homogenisation, these clusters were broken into smaller fragments ( $< 5 \mu\text{m}$ ) (Fig. 4b), resulting in a light-green, almost transparent suspension. The mechanical treatment is expected to supply enough energy to the system to break the membrane structures at the weaker domains and even alter the ultrastructure (stacked, non-stacked conformation). According to the size distribution analysis of the homogenized thylakoid dispersion (Fig. 4b), the resulting thylakoid fragments include membrane domains and protein clusters surrounded by lipids (Fig. 4c).

The structure of the membrane fragments is probably dominated by the hydrophobic interactions between the lipid's hydrophobic tail and hydrophobic protein domains or by lipid/lipid and protein/lipid ionic interactions and hydrogen bonding, similar to the interactions occurring in the native thylakoid membranes.<sup>7,23</sup> These strong interactions prevent the

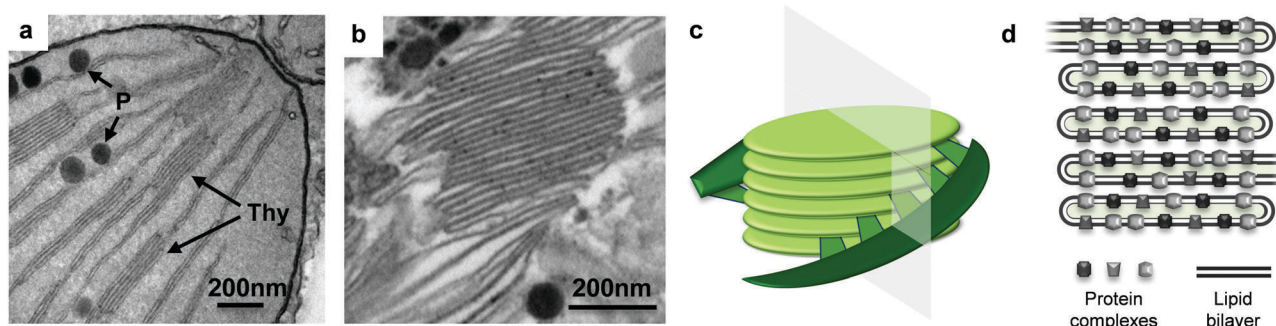


**Fig. 2** TEM micrographs. (a) Leaf cross section focused on a chloroplast portion, thylakoid membranes (Thy) and plastoglobules (P) are identified with the arrows. (b) Thylakoid extract from sugar beet leaves, focused on a grana structure. (c) 3D schematic model of thylakoid grana structure, adapted from Ruban & Johnson.<sup>1</sup> The plane denotes a transversal cut, which is normally observed with TEM micrographs. (d) A cartoon of the transversal view of the thylakoid grana.





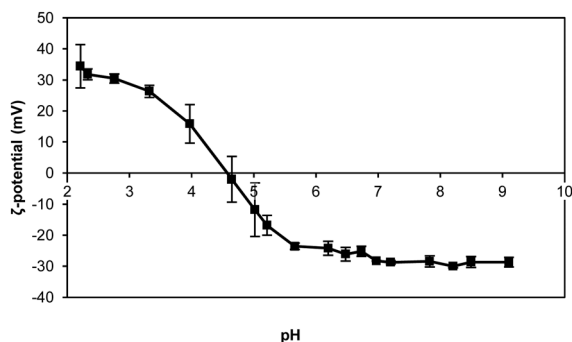


Fig. 3  $\zeta$ -Potential of thylakoid extract upon pH change. Thylakoid membranes were extracted from sugar beet leaves.  $n = 3$ .

release of lipids from the proteins upon membrane disruption and yield protein/lipid complexes. Nevertheless, lipids that were indeed detached can still bind to membrane proteins, which offer a complementary amphipathic surface. These types of interactions are described for protein-surfactant mixtures and are thermodynamically more favourable than micelles.<sup>24</sup> Thus, complexes between proteins and lipids are expected to account for the majority of the thylakoid fragments obtained through homogenisation. The proteins in these fragments can include large protein clusters, since the densely packed protein complexes in thylakoid membranes can arrange in super and megacomplexes mediated by pigments and small proteins.<sup>25</sup>

In addition to the particle size, the micrographs facilitated the identification of the liquid-crystalline structure of the membrane lipids, which were observed as bright spots under polarised light (Fig. 4a and b). Following mechanical rupture, crystalline structures were still observed, although at smaller sizes. Lipid crystal structures in thylakoid membranes include lamellar bilayers, together with hexagonal and cubic phases. The bilayer is a planar structure whereas the hexagonal phase consists of cylindrical inverted micelles packed on an hexagonal lattice.<sup>26</sup> The cubic phase is a bicontinuous structure also formed by inverted micelles with fatty acyl chains pointing toward the outside of tubules and the polar head groups toward the centre.<sup>27,28</sup> The type and amount of membrane lipids and protein complexes determine the crystal conformation adopted by the lipids.<sup>26,27</sup> These crystal structures are expected to be

formed by the lipids surrounding the protein complexes upon thylakoid homogenisation, given the crystals observed in the homogenised material.

### Surface tension

The proteins forming the thylakoid membranes, and now the thylakoid fragments, are membrane spanning proteins. These proteins are rich in hydrophobic domains that can facilitate the adsorption at air–water and oil–water interfaces and contribute to a significant reduction of the interfacial tension. To characterise the interfacial properties of thylakoid membranes, their behaviour at the air–water interface was measured with a Wilhelmy plate during a 4 h period (Fig. 5a). The higher the thylakoid concentration, the lower the final value, ranging from 43.3 to 31.5 mN m<sup>-1</sup> at 0.01 and 0.25 w/v%, respectively (Fig. 5b). At higher thylakoid concentration (>0.25 w/v%), thylakoid fragments started to precipitate, probably due to aggregation.

All tested concentrations (0.01, 0.06, 0.13 and 0.25 w/v%) showed a similar pattern of rapid initial decline which then slows down, reaching a semi-equilibrium at the end of the measurement. This is expected when larger entities, such as the thylakoid fragments, adsorb to an interface. Due to the mechanical homogenisation of the thylakoids, the proteins are part of small membrane fragments consisting of both proteins and lipids. These lipids can surround the proteins and cover the hydrophobic domains,<sup>28</sup> producing stable thylakoid fragments that behave like soft particles at the air–water interface. As soft particles, the thylakoid fragments lower the surface tension due to capillary forces rather than conformational changes at the interface. In particle-stabilised interfaces, lateral attractive capillary forces occur due to deformation of the fluid interface around the particles. Such interactions contribute to the mechanical stability of the interfacial layer.<sup>29</sup>

### Dynamic interfacial tension

The interfacial activity of thylakoid membranes at the oil–water interface was measured to assess their adsorption kinetics (Fig. 6). Measurements were done for 24 h with a pendant drop analysis at a thylakoid concentration of 0.001 w/v%. When looking at the logarithmic time scale used in Fig. 6a, three phases of surface adsorption can be identified. These phases have been

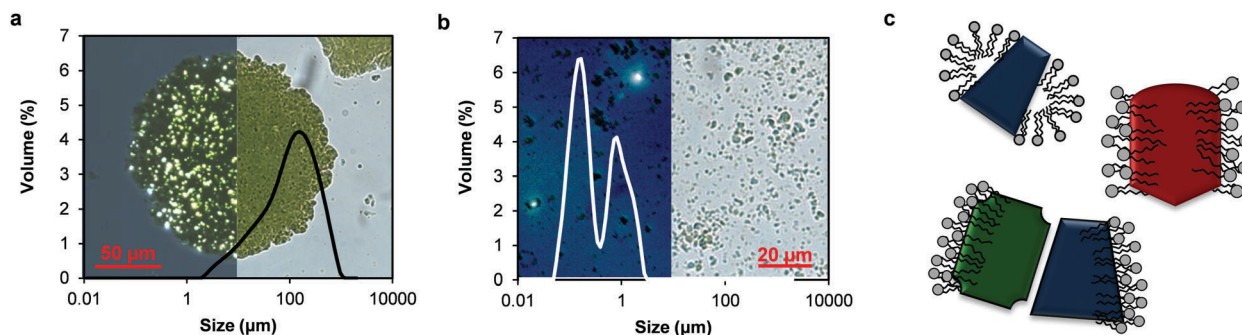


Fig. 4 Comparison of thylakoid extract before (a) and after (b) homogenisation. The background of the graphs are light microscope images with and without light polarisation. (c) Proposed structures of the thylakoid membrane fragments: membrane domains and protein clusters surrounded by lipids.

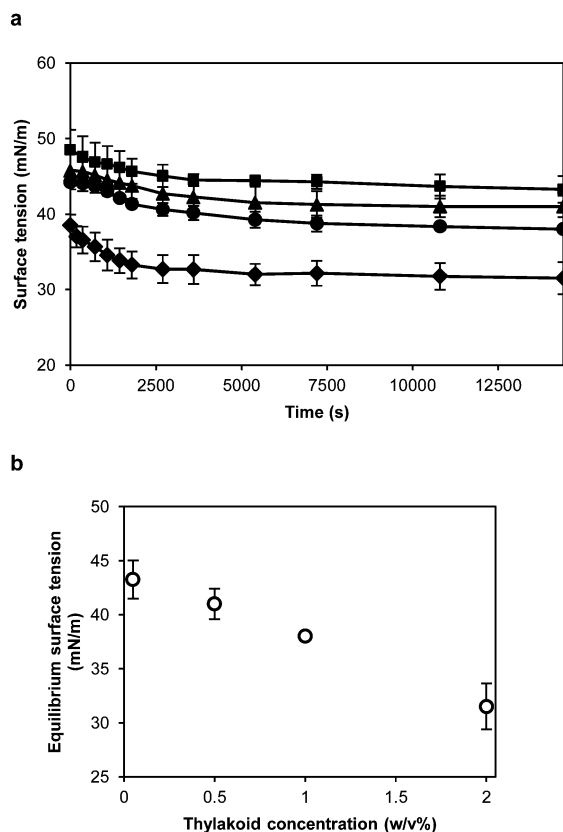


Fig. 5 (a) Surface tension of the air–water interface of thylakoid dispersions at different concentrations: (■) 0.01 w/v%, (▲) 0.06 w/v%, (●) 0.13 w/v%, and (◆) 0.25 w/v%, all in dry basis. (b) Final surface tension as a function of concentration of the thylakoid fragments.  $n = 3$ .

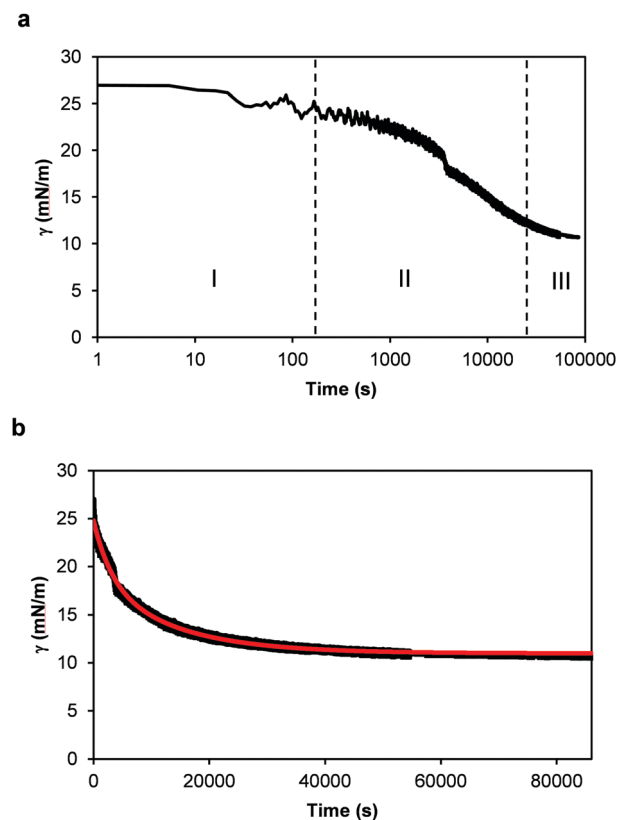


Fig. 6 Dynamic surface tension ( $\gamma$ ) measurements of 0.001 w/v% thylakoid solution as a function of time. (a) Time expressed using a time logarithmic scale. I, II and III indicate the three phases of diffusion, adsorption and finally rearrangement and equilibrium, as defined for single proteins. And (b) time in linear scale. In red: theoretical curve using eqn (1).

observed in most cases where proteins have been used as stabilisers<sup>30</sup> and an analogy can be identified for the thylakoid fragments. In the first phase (I), the thylakoid fragments have not reached the interface yet and the interfacial tension remains constant. The second phase (II) describes the adsorption of thylakoid fragments to the interface, characterized by the main decrease in interfacial tension. Finally, during the third phase (III) interactions between the adsorbed fragments lower the interfacial tension to an equilibrium value. The measurements done on the air–water surface fit phase II and therefore show similar kinetics. This suggests that the same type of adsorptive process takes place there as well.

Similar adsorption kinetics have been observed for globular proteins (*i.e.* lipases, glutamate dehydrogenase),<sup>30</sup>  $\beta$ -casein<sup>31,32</sup> and for oleosins.<sup>33</sup> In all cases, the equilibrium interfacial tension is reached after  $\sim 20$  h, except for oleosins ( $\sim 7$  h). Long times for adsorption are common for complex proteins,<sup>34</sup> but also for soft particles that are surface active.<sup>35,36</sup> As indicated earlier, the thylakoid fragments as expected to consist of membrane proteins covered by lipids, which can provide a stable conformation to the protein/lipid complexes and render a soft particle that adsorbs to the interface.

During the pendant drop analysis, the protein hydrophobic groups are partly covered by the surrounding lipids and partly

exposed to the oil–water interface. Once at the interface, new non-covalent bonds are formed, and possibly new bridges and interactions. This process is often irreversible and results in closely-packed, cross-linked, gel-like structures at the interface.<sup>37</sup> During adsorption of the thylakoid fragments, the membrane lipids play an important role. As single amphiphiles, lipids can displace proteins from the interface because they are effective surface-active substances and lower the interfacial tension more than proteins do.<sup>34,38</sup> This displacement will depend on the concentration of both lipids and proteins. A lipid-controlled adsorption occurs much faster than with proteins and should result in a quick lowering of the interfacial tension. However, no decrease of interfacial tension was observed during the first seconds of analysis with the thylakoid fragments (Fig. 6a), suggesting that the thylakoids lipids are somehow not available to freely adsorb to the oil–water interface. This observation supports the idea that thylakoid fragments behave as intact particles and most of lipids remain complexed within this system.

To further analyse the interfacial behaviour of the thylakoid fragments, the interfacial tension was plotted against a linear time scale (Fig. 6b). Similar to the surface tension measurements, the interfacial tension decreased before reaching a plateau value. The thylakoids lowered the interfacial tension

to  $\sim 10 \text{ mN m}^{-1}$ , similar to values obtained by large proteins like ovalbumin,<sup>39</sup>  $\beta$ -lactoglobulin,  $\beta$ -casein and human serum albumin.<sup>40</sup>

Finally, the experimental data in Fig. 6b was fitted well by (1) as depicted by the red line. The relaxation times  $t_1$  and  $t_2$  were equal to 13 250 s and 3058 s, respectively, with a coefficient of determination ( $r^2$ ) of 0.9916. These parameters describe the interfacial tension decay with time and they give an indication of the contributions of adsorption and rearrangement to the dynamic surface tension. In this case,  $t_1$  was four times larger than  $t_2$ , suggesting a relatively slow adsorption compared to fast arrangements of fragments at the interface. Certainly, the large sizes of the thylakoid fragments determined a slow diffusion and adsorption, typical of large molecules or soft particles, resembling Pickering emulsifiers.

### Surface elasticity and viscosity

Dilatational rheology measurements were made after 24 h adsorption time of the thylakoid fragments at the oil–water interface to study the interfacial structure and interactions between adsorbed molecules. Fig. 7a presents plots of the interfacial dilatational elastic ( $E_d'$ ) and viscous ( $E_d''$ ) moduli *versus* angular frequency. The values of the moduli were dependent upon the applied frequency, meaning that the adsorbed thylakoid layer at the oil–water interface had viscoelastic properties.<sup>41</sup> The  $E_d''$  was negligible compared to  $E_d'$ , indicating that the adsorbed layer exhibited pure elastic behaviour.

Before oscillations started, the elastic modulus was  $\sim 10 \text{ mN m}^{-1}$  and increased with the drop deformation rate up to  $23.3 \text{ mN m}^{-1}$ .

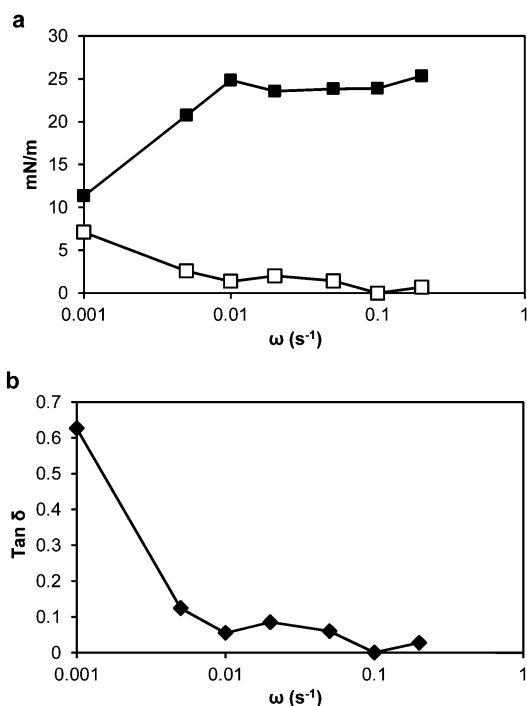


Fig. 7 (a) Interfacial dilatational elastic  $E_d'$  (■) and viscous  $E_d''$  (□) moduli, and (b) loss tangent as a function of oscillation frequency with a 0.03 w/v% thylakoid solution ( $T = 25^\circ\text{C}$ , amplitude = 5% of the initial drop volume).

Above a frequency of  $0.02 \text{ s}^{-1}$ , the elastic modulus reached a plateau at  $\sim 23 \text{ mN m}^{-1}$ . This behaviour suggests that the adsorbed layer formed a mechanically stable structure.

The dynamic viscoelastic behaviour can be analysed more intuitively with the loss tangent ( $\tan \delta$ ), which is equal to  $E_d''/E_d'$ . When  $\tan \delta > 1$ ,  $E_d''$  is dominant and the interface mainly exhibits viscous properties. In contrast, when  $\tan \delta < 1$ , the interface mainly exhibits elastic properties. In our system, the  $\tan \delta$  was below 1 at all frequencies and from  $0.01 \text{ s}^{-1}$ , with low frequency dependence (Fig. 7b). Thus, the surface elasticity had a greater contribution to the dilatational modulus than the surface viscosity. Between the thylakoid fragments, the protein/protein, protein/lipid and lipid/lipid interactions will take place at the interface and result in an elastic interfacial film or 2D network, which can show viscoelastic response to mechanical disturbances.<sup>42,43</sup>

### Thylakoid stabilised emulsions

The interfacial properties of thylakoid membranes can be related to their emulsifying activity, as it has been done for proteins<sup>41</sup> and hydrocolloids.<sup>44</sup> Therefore, oil-in-water emulsions were prepared with homogenized thylakoid extract at different concentrations. Two phases were observed at all concentrations due to size dispersity of the oil droplets and/or aggregates of droplets (Fig. 8). The droplet size indeed showed a bimodal distribution (Fig. 9); however, the majority of the droplets had small size at all concentrations, as observed in the micrographs (backgrounds in Fig. 9). The large oil droplets are due to slow diffusion of the thylakoids fragments, which cannot efficiently stabilise all the newly created interface during emulsion formation. This behaviour suggests similarities between thylakoid fragments and soft particles or Pickering emulsifiers. Furthermore, droplet aggregates were observed at increasing thylakoid concentrations. The aggregates resulted in peaks at large particle size ( $\sim 100 \mu\text{m}$ ) (Fig. 9b) and in a larger top phase in the emulsions (Fig. 8).

To further characterise the colloidal stability of the emulsions, the  $\zeta$ -potential was measured as a function of pH (Fig. 10). The IEP was found at pH 5.1, higher than for the pure thylakoid

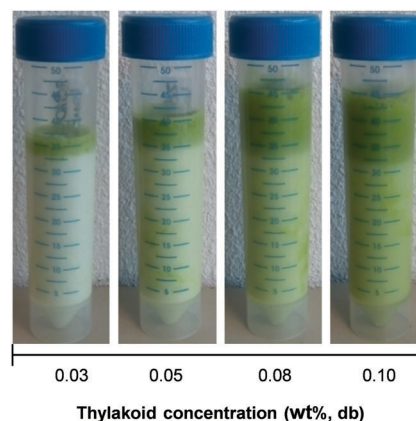


Fig. 8 Visual appearance of oil-in-water emulsions stabilised by thylakoid extract at different concentrations. Pictures were taken right after emulsions preparation.



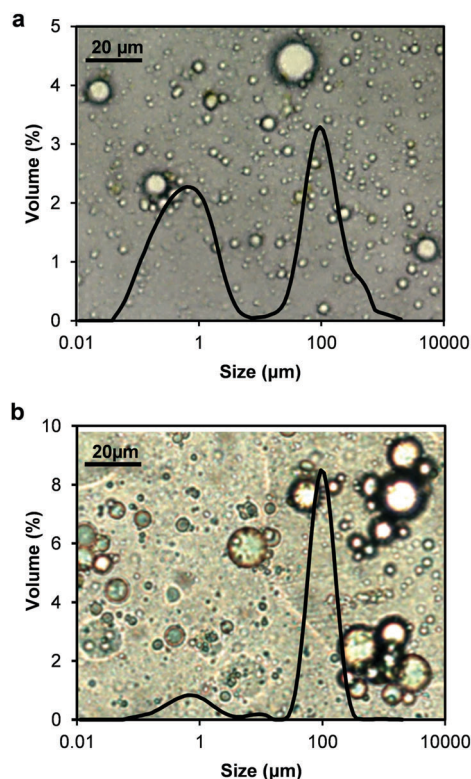


Fig. 9 Optical micrographs combined with their respective oil droplet-size distributions obtained by laser light diffraction of thylakoid-stabilized o/w emulsions after dilution of 1 : 100. (a) 0.05 w/v% and (b) 0.1 w/v% thylakoids.

solution (pH 4.7), but the charge range was similar ( $\pm 30$  mV). The change of the IEP suggests re-arrangement of the proteins and lipids in the thylakoid fragments. Upon homogenisation, the resulting protein/lipid complexes had a different distribution of charges around protein complexes that induced an IEP shift.

At the emulsion conditions (pH 6.8), the oil droplets covered with thylakoids are expected to repel each other due to the negative charge that is exposed at this pH. However, having droplet aggregates at this pH suggests that the attractive forces are stronger than the electrostatic repulsion and aggregation occurs, probably in a similar manner as thylakoid membranes stack on top of each other in the native structure. In the emulsion system, the exposed negative charges on the thylakoid fragments, together with the available multivalent cations, can balance the electrostatic repulsion and facilitate the inter droplet interactions. Additionally, emulsions prepared at different pH conditions (pH 3.0, 4.7, and 7.0) showed similar properties and stability (data not shown) as the emulsions at pH 6.8. This observation confirmed that electrostatic interactions played no major role on the stabilisation mechanism. Instead, stabilising forces on the interface and bulk phase might be ruled by hydrophobic and van der Waals' interactions, which can contribute to stability of the interfacial layer as well as bridging of droplets. Moreover, the attractive interactions between droplets might be enhanced by small thylakoid fragments that can induce depletion flocculation and contribute to phase separation of the emulsions.

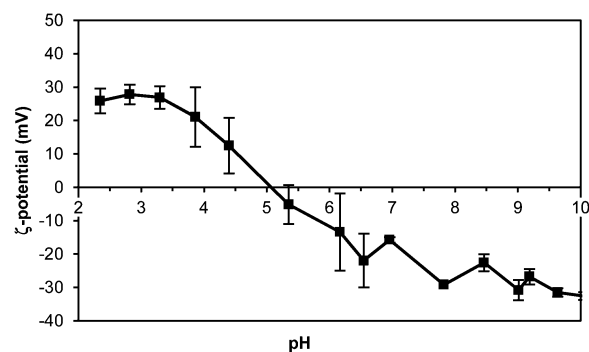


Fig. 10  $\zeta$ -Potential of thylakoid stabilised emulsion upon pH change. 0.05 w/v% thylakoid solution.  $n = 3$ .

Despite the droplet aggregation, the thylakoid emulsions were stable against coalescence over time. The average diameter  $d_{43}$  did not increase over 7 days of storage (Fig. 11) and no free oil was observed on the emulsion's surface. The aggregation of droplets occurred already during emulsion preparation and the droplet clusters remained stable. This immediate aggregation might be caused by insufficient thylakoid fragments to saturate the droplet surface. In that case, the insufficient adsorbed molecules are shared between droplets and steric bridging occurs. Such bridging flocculation during emulsification has been described for single proteins (*i.e.* lactoglobulin) and an increase on protein concentration reduced droplet aggregation.<sup>45</sup> Nevertheless, the increase of thylakoid concentration resulted in even more aggregation. Most likely, multiple layers of thylakoids were formed at the interface due to the excess of material and the electrostatic bridging between droplets was probably promoted. Since the thylakoids have a natural tendency to stack, one may expect that this also happens on an interface. A stack of thylakoids can then easily form a bridge towards neighbouring droplets, resulting in aggregation.

After droplet aggregation, the adsorbed thylakoid fragments might form lateral interactions as part of the structural consolidation of the adsorbed layer. These interactions result in a 2D network around the oil droplets that ultimately stabilises the emulsion against coalescence over time.

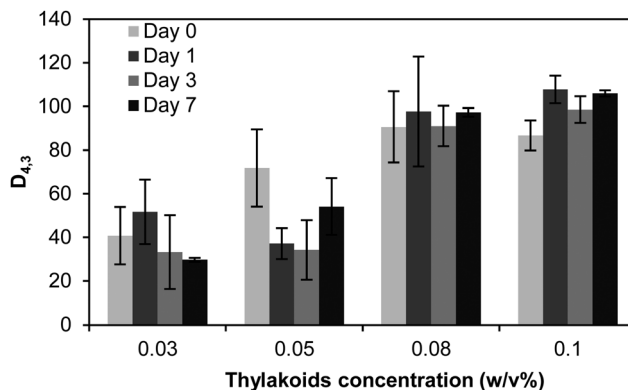


Fig. 11 Average droplet size diameter  $d_{43}$  of emulsions stabilised by thylakoid solutions at different concentrations and after 7 days of storage at 4 °C.  $n = 3$ .



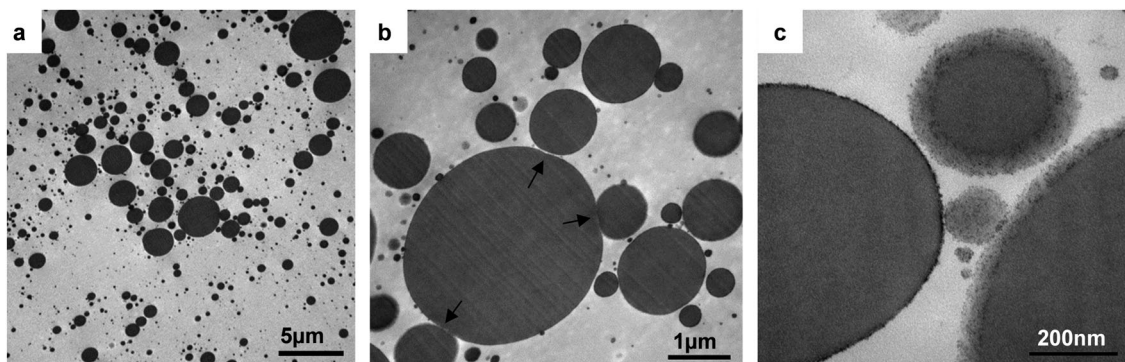


Fig. 12 TEM micrographs of thylakoid stabilised emulsion at different magnification levels. (a) size polydispersity of oil droplets. (b) Zoom-in on a cluster of droplets; the arrows point at local flattening of the droplets, probably due to surface deformation upon droplet aggregation. (c) Zoom-in on a droplet edge.

A thylakoid stabilised emulsion was analysed with the aid of TEM (Fig. 12) to visualise the emulsion droplets and the thylakoid structures after emulsification. The size polydispersity of oil droplets and droplet aggregates are depicted in Fig. 12a and b, respectively. Aggregates contained small droplets with local flattening of the surface (see arrows) due to the elasticity of the adsorbed thylakoid layer, which deforms upon attraction. The local flattening may indicate a very strong bridging; strong enough to deform the droplets and hence enlarge their surface area. The elastic properties of the adsorbed layer were described during the dilatational rheology analysis of the thylakoids, suggesting the formation of a 2D network with viscoelastic response. The resulting surface flattening upon droplet aggregation can enhance the attractive forces between droplets.<sup>38</sup> However, no coalescence was observed after droplet aggregation, confirming the mechanical stability of the adsorbed layer.

Moreover, no intact thylakoid structures were observed when using higher magnification level (Fig. 12c), which was the same magnification level used to visualise the thylakoid extract in Fig. 2b. Interestingly, no thylakoid vesicles stuck out of the droplets as previously described by Rayner, *et al.*<sup>8</sup> when thylakoid-stabilised emulsions were tested. The different thylakoid isolation method and emulsion preparation might account for this major difference. In particular, the homogenisation step was done at higher pressure in our case (150 bar compared to 100 bar), and this high pressure can lead to more breakage of the thylakoid ultrastructure. Instead of having intact thylakoid domains reaching the oil–water interface, small thylakoid fragments adsorbed at the interface and formed a thin covering layer. This covering layer can be the cause for the smeared edges of the oil droplets in the close-up image (Fig. 12c). The smeared layer had a thickness of 30–50 nm, suggesting the adsorption of multiple layers since the thickness of lamellar thylakoids is ~10 nm. Those observations confirm the tendency of the thylakoids to stack. The presence of multiple adsorbed layers promotes bridging between droplets either by steric or electrostatic bridging, which was confirmed by the immediate aggregation of droplets during emulsification even at higher thylakoid concentrations.

Additionally, the black dots or small droplets (10–80 nm) observed in the emulsions had comparable sizes to the plastoglobules identified in the thylakoid extract and in the homogenised material. These thylakoid microdomains have a diameter ranging between 30–100 nm and are assumed to remain in suspension after emulsion preparation due to their stable conformation and due to interface crowding by thylakoid fragments.

### Emulsifying mechanism

Fig. 13 depicts a proposed mechanism of thylakoid fragment adsorption at the oil–water interface. The lipids in the thylakoid fragments cover the hydrophobic patches of the protein complexes and thereby provide a stable conformation to the membrane proteins. The strong interactions between the lipids and proteins result in fragments that behave more like soft particles at the interface, impeding the individual adsorption of either the proteins or the lipids. During emulsification, bridging flocculation of thylakoid-covered droplets occurs through electrostatic interactions similar to those in thylakoid stacking and hydrophobic interactions. Over time, the adsorbed thylakoid fragments form new interactions that result in an elastic and stable 3D network. This 3D network ensures long time stability against coalescence, since the oil droplets are immobilised within a gel-like film with elastic properties.<sup>43</sup>

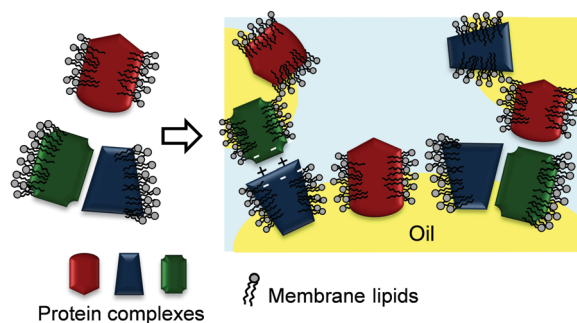


Fig. 13 Proposed emulsifying mechanism of thylakoid membrane fragments.



## Conclusions

In this work we have studied the interfacial behaviour of thylakoid membranes to discern the adsorption mechanism and the ability to stabilise oil–water interfaces. Thylakoid membranes are unique biological membranes with a high protein/lipid ratio, a special lipid composition and specific protein/lipid interactions. The thylakoid proteins and their intrinsic lipids form stable thylakoid fragments that behave like soft particles during adsorption and interface stabilisation. In emulsions, the adsorbed thylakoid fragments form an elastic network around oil droplets and render an emulsion stable against coalescence, despite aggregation of droplets by bridging. The droplet aggregation is proposed to be promoted by the natural tendency towards stacking of the native thylakoid membranes. Both composition and structure of thylakoid fragments determine their emulsifying properties and make the interfacial behaviour more complex compared to artificial protein/lipid mixtures. The emulsion stability obtained with thylakoid fragments can be further explored in specialised applications of encapsulation systems, where the search for natural materials is gaining more attention.

## Acknowledgements

The authors thank Jun Qiu for his contribution to the data fitting in MATLAB, and the Technology Foundation STW (The Netherlands) and Royal Cosun (The Netherlands) for their financial and project support.

## References

- 1 A. V. Ruban and M. P. Johnson, *Nat. Plants*, 2015, **1**, 15161.
- 2 S. Rottet, C. Besagni and F. Kessler, *Biochim. Biophys. Acta, Bioenerg.*, 2015, **1847**, 889–899.
- 3 R. Nevo, S. G. Chuartzman, O. Tsabari, Z. Reich, D. Charuvi and E. Shimoni, *Lipids in photosynthesis*, Springer, 2009, pp. 295–328.
- 4 S. G. Sprague, *J. Bioenerg. Biomembr.*, 1987, **19**, 691–703.
- 5 L. A. Staehelin and G. W. van der Staay, in *Oxygenic photosynthesis: The light reactions*, Springer, 1996, pp. 11–30.
- 6 H. Kirchhoff, U. Mukherjee and H. J. Galla, *Biochemistry*, 2002, **41**, 4872–4882.
- 7 B. Loll, J. Kern, W. Saenger, A. Zouni and J. Biesiadka, *Biochim. Biophys. Acta, Bioenerg.*, 2007, **1767**, 509–519.
- 8 M. Rayner, H. Ljusberg, S. C. Emek, E. Sellman, C. Erlanson-Albertsson and P.-Å. Albertsson, *J. Sci. Food Agric.*, 2011, **91**, 315–321.
- 9 C. Erlanson-Albertsson and P. Å. Albertsson, *Plant Foods Hum. Nutr.*, 2015, **70**, 281–290.
- 10 K. Östbring, M. Rayner, P. A. Albertsson and C. Erlanson-Albertsson, *Food Funct.*, 2015, **6**, 1310–1318.
- 11 A. Tamayo Tenorio, J. Gieteling, G. A. H. de Jong, R. M. Boom and A. J. van der Goot, *Food Chem.*, 2016, **203**, 402–408.
- 12 C. Berton, C. Genot and M. H. Ropers, *J. Colloid Interface Sci.*, 2011, **354**, 739–748.
- 13 A. P. Casazza, D. Tarantino and C. Soave, *Photosynth. Res.*, 2001, **68**, 175–180.
- 14 D. Joly and R. Carpentier, *Photosynthesis Research Protocols*, Springer, 2011, pp. 321–325.
- 15 AACC, *Approved Methods of Analysis*, 10th edn, AACC International, St. Paul, MN, USA, 1983.
- 16 AACC, *Approved Methods of Analysis*, 10th edn, AACC International, St. Paul, MN, USA, 1983.
- 17 AACC, *Approved Methods of Analysis*, 10th edn, AACC International, St. Paul, MN, USA, 1983.
- 18 M. Pribil, M. Labs and D. Leister, *J. Exp. Bot.*, 2014, **65**, 1955–1972.
- 19 R. Fristedt, P. Granath and A. V. Vener, *PLoS One*, 2010, **5**, e10963.
- 20 G. Finazzi, D. Petroustos, M. Tomizioli, S. Flori, E. Sautron, V. Villanova, N. Rolland and D. Seigneurin-Berny, *Cell Calcium*, 2015, **58**, 86–97.
- 21 B. Demé, C. Cataye, M. A. Block, E. Maréchal and J. Jouhet, *FASEB J.*, 2014, **28**, 3373–3383.
- 22 H.-E. Åkerlund, B. Andersson, A. Persson and P.-Å. Albertsson, *Biochim. Biophys. Acta, Bioenerg.*, 1979, **552**, 238–246.
- 23 P.-A. Siegenthaler and A. Trémolières, in *Lipids in Photosynthesis: Structure, Function and Genetics*, ed. S. Paul-André and M. Norio, Springer, Netherlands, Dordrecht, 1998, pp. 145–173.
- 24 M. N. Jones, *Chem. Soc. Rev.*, 1992, **21**, 127–136.
- 25 J. P. Dekker and E. J. Boekema, *Biochim. Biophys. Acta, Bioenerg.*, 2005, **1706**, 12–39.
- 26 W. P. Williams, in *Lipids in Photosynthesis: Structure, Function and Genetics*, ed. S. Paul-André and M. Norio, Springer, Netherlands, Dordrecht, 1998, pp. 103–118.
- 27 E. Selstam, in *Lipids in Photosynthesis: Structure, Function and Genetics*, ed. S. Paul-André and M. Norio, Springer, Netherlands, Dordrecht, 1998, pp. 209–224.
- 28 J. Jouhet, *Front. Plant Sci.*, 2013, **4**, 494.
- 29 C. C. Berton-Carabin and K. Schroën, *Annu. Rev. Food Sci. Technol.*, 2015, **6**, 263–297.
- 30 C. Beverung, C. Radke and H. Blanch, *Biophys. Chem.*, 1999, **81**, 59–80.
- 31 R. Wüstneck, V. B. Fainerman, E. V. Aksenenko, C. Kotsmar, V. Pradines, J. Krägel and R. Miller, *Colloids Surf., A*, 2012, **404**, 17–24.
- 32 A. Dan, R. Wüstneck, J. Krägel, E. V. Aksenenko, V. B. Fainerman and R. Miller, *Food Hydrocolloids*, 2014, **34**, 193–201.
- 33 C. V. Nikiforidis, C. Ampatzidis, S. Lalou, E. Scholten, T. D. Karapantsios and V. Kiosseoglou, *Soft Matter*, 2013, **9**, 1354–1363.
- 34 Q. He, Y. Zhang, G. Lu, R. Miller, H. Möhwald and J. Li, *Adv. Colloid Interface Sci.*, 2008, **140**, 67–76.
- 35 Z. Li, D. Harbottle, E. Pensini, T. Ngai, W. Richtering and Z. Xu, *Langmuir*, 2015, **31**, 6282–6288.
- 36 A. Boker, J. He, T. Emrick and T. P. Russell, *Soft Matter*, 2007, **3**, 1231–1248.



- 37 V. Mitropoulos, A. Mütze and P. Fischer, *Adv. Colloid Interface Sci.*, 2014, **206**, 195–206.
- 38 P. Walstra, in *Physical Chemistry of Foods*, Marcel Dekker Inc., USA, 2003, ch. 10.
- 39 L. Seta, N. Baldino, D. Gabriele, F. R. Lupi and B. de Cindio, *Food Hydrocolloids*, 2012, **29**, 247–257.
- 40 G. Lu, H. Chen and J. Li, *Colloids Surf., A*, 2003, **215**, 25–32.
- 41 A. Williams and A. Prins, *Colloids Surf., A*, 1996, **114**, 267–275.
- 42 E. Dickinson, *Trends Food Sci. Technol.*, 2012, **24**, 4–12.
- 43 E. Dickinson, *J. Sci. Food Agric.*, 2013, **93**, 710–721.
- 44 E. Dickinson, *Food Hydrocolloids*, 2009, **23**, 1473–1482.
- 45 H. J. Kim, E. A. Decker and D. J. McClements, *Langmuir*, 2004, **20**, 10394–10398.

